

Nanofluid and ferrofluid slip flow in rectangular and circular microchannels and minichannels

Abstract. This paper has developed a formulation of fluid motion and entropy production in microchannels. We have developed the formulations for pressure driven flow, flow under electric forces and flow under ferromagnetic forces. Friction, thermal and electromagnetic irreversibilities have significance in energy efficiency of microfluid systems. The results indicate that entropy and the Second Law have practical significance in electrokinetic liquid transport through microchannels.

Streszczenie. W artykule pokazano rozwój sformułowania ruchu płynu i entropii produkowanej w mikrokanalikach. Rozwinięte zostały sformułowania dla przepływów poddanych ciśnieniu, przepływów w polu elektrycznym i przepływów poddanych siłom ferromagnetycznym. Ciśnienie, cieplna i elektromagnetyczna nieodwracalność mają istotne znaczenie dla efektywności energetycznej systemów mikroprzepływnych. Wyniki wskazują, że entropia i drugie prawo termodynamiki mają praktyczne znaczenie w transporcie płynów elektrokinetycznych przez mikrokanaliki. (Nano- i ferropłyny w kołowych i prostokątnych mikro- i mini kanalikach)

Keywords: ferrofluids, magnetohydrodynamics, microchannel flow.

Słowa kluczowe: ferrofluidy, magnetohydrodynamika, przepływ mikrokanalowy.

Introduction

Fluid flows through microchannels and capillaries of different geometries arise in various emerging technologies, ranging from electronics cooling [1] to slip-flow control [2] and others [3]. In electronics cooling applications, past analytical methods have been developed to predict Nusselt number variations in microchannels of various aspect ratios [1]. Past studies have different views regarding the apparent viscosity in microchannel flows [4 – 6]. In certain cases, the apparent (required or measured) viscosity is reported to be much larger than the bulk viscosity at large distances away from the wall (Israelachvili; [4]). However, in other studies conducted with flows in capillaries, the apparent and bulk viscosities are nearly equal (Anderson, Quinn; [5]). Additional data for capillaries smaller than a micron in diameter was reported by Migun and Prokhorenko [6]. Pfahler et al. [7] give experimental data indicating that the apparent viscosity is smaller than the bulk viscosity of various liquids in microchannels (isopropyl alcohol, alcohol). The authors reported data for the liquid flow rate as a function of microchannel size, type of fluid and pressure drop across the microchannel. A criterion involving the lateral wall influence on the microchannel flow rate was documented by Sharipov [8]. Rarefaction parameters at the ends of the microchannel were related to the mass flow rate.

Experimental data regarding liquid flows in microchannels with hydraulic diameters between 30 and 344 microns was reported by Xu et al. [9]. The range of Reynolds number lied between 20 and 4,000. Their results indicate that flow characteristics agree with analogous behavior predicted by the Navier – Stokes equations in the same range of Reynolds number. Other studies have shown that heat transfer reduces frictional losses in microchannels, particularly at low Reynolds numbers [10]. At lower Reynolds numbers and temperatures, the fluid viscosity decreases and the wall friction becomes smaller. Such data was reported for three-dimensional flow variations of steady, laminar flow in a microchannel [10]. A relative temperature difference between the fluid and solid phases has been used to check the validity of local thermodynamic equilibrium assumptions in microchannels (Kim, Kim, Lee; [11]).

Velocity distribution in rectangular and circular microchannels

Fluid flow in microchannels is driven due to presence of electric field, magnetic field or pressure driven flow (Fig1). In the first case flow transport is initiated by application of a

high electric field (magnetohydrodynamics MHD), in the second case fluid flow is driven due to strong forces of magnetic polarization (ferrohydrodynamics (FHD), in the last case, flow is transported by pressure differential (pressure hydrodynamics PHD))

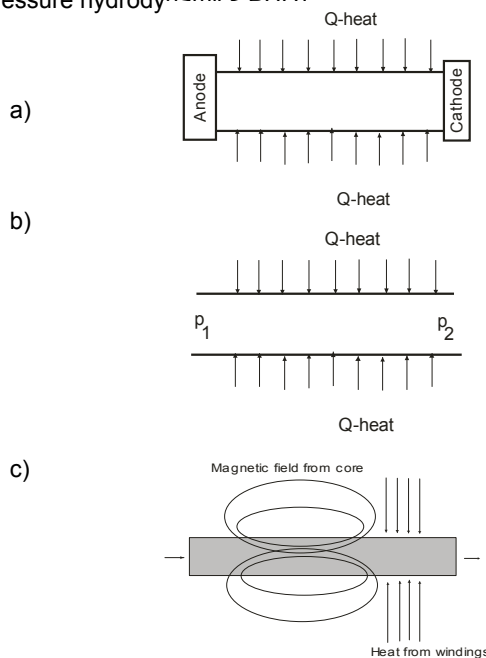


Fig. 1: Types of fluid flow: a-magnetohydrodynamics(MHD), b-pressurehydrodynamics (PHD), c-ferrohydrodynamics (FHD)

Consider elektrokinetic flow in rectangular and circular microchannels (Fig. 2). The charged surface of a microchannel wall may attract ions of the opposite charge in the surrounding fluid. The general form of the momentum equation for electrohydrodynamic flow is:

$$(1) \quad \rho \frac{\partial \vec{v}}{\partial t} + \rho \vec{v} \cdot \nabla \vec{v} = -\nabla p + \nabla(\mu \nabla \vec{v}) + \vec{i} \times \vec{B},$$

where the last term represents the electromagnetic force and i and B refer to the current density and magnetic field strength, respectively. For steady-state flow in a microchannel at small Reynolds numbers, the transient and inertia terms can be neglected, so Eq. (1) is simplified as follows:

$$(2) \quad 0 = -\nabla p + \nabla(\mu \nabla \vec{v}) + \vec{i} \times \vec{B},$$

Influence of electro-thermomagnetic field in a rectangular microchannel

Electro-thermomagnetic effects on microfluidic transport have been reported previously in Refs. [17 – 20]. During elektrokinetic flow in microchannels, the charged surface of a microchannel wall may attract ions of the opposite charge in the surrounding fluid. The resulting spatial gradient of ions near the wall leads to an Electric Double Layer (EDL). The EDL contains an immobile inner layer and mobile outer layer, which can be appreciably affected by an externally applied electric field. Assuming the fluid velocity, magnetic field and current density are orthogonal, the reduced momentum equation becomes:

$$(3) \quad 0 = -\frac{dp}{dx} + \eta \frac{d^2u}{dz^2} + i_y B_z$$

The terms represent pressure, viscous and electromagnetic forces in the liquid. Using Ohm's Law to express the current density in terms of fluid velocity:

$$(4) \quad \eta \frac{d^2u}{dz^2} + \sigma_e B_z^2 u = \frac{dp}{dx},$$

where σ_e and B_z refer to the electrical conductivity and magnetic field strength. For fully developed flow in a microchannnel, the pressure gradient becomes constant and independent of the magnetic field strength. In terms of the Hartman number, M_H ($M_H = aB_z \sqrt{\sigma_e/\eta}$),

$$(5) \quad \eta \frac{d^2u}{dz^2} - \left(\frac{M_H^2 \eta}{a^2} \right) u = \frac{dp}{dx}$$

Applying the no-slip boundary conditions at $z=0$ and $z=-2a$, the analytical solution of Eq. (5) becomes:

$$(6) \quad u = -\frac{a^2 \left(\frac{dp}{dx} \right)}{M_H^2 \mu} + \frac{a^2 \left(\frac{dp}{dx} \right)}{(1+2e^{2M_H}) M_H^2 \mu} e^{\frac{z-M_H}{a}} + \frac{a^2 \left(\frac{dp}{dx} \right) e^{2M_H}}{(1+2e^{2M_H}) M_H^2 \mu} e^{-\frac{z-M_H}{a}}$$

The mean velocity within the microchannel becomes:

$$(7) \quad u_b = \frac{1}{2a} \int_0^{2a} u(z) dz$$

Non-dimensionlizing this result ($z^* = z/a$, $u^* = u/u_b$),

$$(8) \quad u^* = \frac{M_H \left(-1 + \frac{1}{(1+2e^{2M_H})} e^{z^* M_H} + \frac{e^{2M_H}}{(1+2e^{2M_H})} e^{-z^* M_H} \right)}{(-M_H + \tanh(M_H))}$$

Without electromagnetic effects, equation (11) transforms into the following expressions:

$$(9) \quad u(z) = \frac{\left(\frac{dp}{dx} \right)}{2\mu} (-2az + z^2)$$

$$(10) \quad u_b = \frac{1}{2a} \int_{-a}^a u(z) dz = \frac{a^2 \left(\frac{dp}{dx} \right)}{3\mu}$$

$$(11) \quad u^* = \frac{3}{2} (2 - z^*) z^*$$

For the circular microchannel, the governing equation is:

$$(12) \quad \frac{dp}{dx} = \mu \left(\frac{\partial^2 u}{\partial r^2} + \frac{1}{r} \frac{\partial u}{\partial r} \right)$$

Solving the differential equation subject to boundary conditions,

(13)

$$u = \frac{\left(\frac{dp}{dx} \right)}{4\mu} (r^2 - R^2)$$

(14)

$$u_b = \frac{1}{\pi R^2} \int_0^R v 2\pi r \cdot dr = -\frac{\left(\frac{dp}{dx} \right) R^2}{8\mu}$$

(15)

$$u^* = 2 - 2r^*{}^2$$

Previous investigations of the pressure gradient for electroosmotic liquid flow in microchannels have generally used no-slip conditions, while for gas flow in microchannels, the slip boundary condition is taken into account. Some previous experimental investigations have demonstrated the existence of liquid slip on a microchannel wall. Also, some previous studies predicted numerically a slip velocity for liquid flow in a microchannel made from hydrophobic surfaces, taking into account an imposed electric field and a pressure gradient without heat transfer. On the basis of a slip velocity profile in liquid microchannel flow, the velocity profile can be determined by:

$$u(0) = u_{s1}, u(2a) = u_{s2}$$

$$u_{s1} = \beta \left. \frac{\partial u}{\partial z} \right|_{z=0}, \quad u_{s2} = \beta \left. \frac{\partial u}{\partial z} \right|_{z=2a}$$

The coefficient β is called the slip coefficient. If we define a reduced slip coefficient as $\beta^* = \beta/a$, we obtain the following equations:

1) Rectangular channel with electromagnetic forces;

(16)

$$u^* = \frac{M_H (\cosh(M_H) - \cosh(M - Mz^*)) - M_H \beta^* \sinh(M_H)}{M_H \cosh(M_H) + (-1 + M_H \beta^*) \sinh(M_H)}$$

Rectangular channel without electromagnetic forces;

$$u^* = \frac{6z^* - 3z^*{}^2 + 6\beta^*}{2 + 6\beta^*}$$

Circular channel without electromagnetic forces;

$$\beta^* = \frac{\beta}{R}, r^* = r/R$$

(17)

$$u^* = 1 + \frac{-2r^*{}^2 + 1}{1 + 4\beta^*}$$

Convective heat transfer formulation and formulation of exergy losses

For convective heat transfer within the microchannel, the transient, inertial and streamwise conduction terms can be neglected for small Reynolds numbers at steady state [17 – 18]. Then the reduced form of the energy equation becomes

$$(18) \quad \lambda \frac{d^2 T}{dz^2} + \eta \left(\frac{du}{dz} \right)^2 + \frac{i_y^2}{\sigma_e} = 0$$

Define the following non-dimensional temperature, θ , and electromagnetic coefficient, C

$$(19) \quad \theta(z^*) = \frac{\lambda(T - T_w)}{\eta u_b^2}$$

$$(20) \quad C = M_H (K - 1) \cosh M_H - K \sinh M_H$$

where K represents a non-dimensional load factor (ratio of the applied electric field strength to the product of the mean velocity, u_b , and magnetic field strength).

In terms of the non-dimensional variables, the energy equation becomes

$$(21) \quad \frac{d^2\theta}{dz^2} = -\left(\frac{du}{dz}\right)^2 - i_y^2$$

The entropy production rate can be expressed as a sum of positive-definite terms corresponding to friction, thermal and electromagnetic irreversibilities, i.e.,

$$(22) \quad \dot{P}_s = \frac{\lambda VIT}{T^2} + \frac{\eta\Phi}{T} + \frac{\sigma_e}{T} (\vec{E} + \vec{v} \times \vec{B}) (\vec{E} + \vec{v} \times \vec{B})$$

In Eq. (22), the terms on the right side represent a sum of squared terms, so the entropy production is positive, thereby complying with the Second Law of Thermodynamics. Based on the assumptions outlined previously in the fluid flow and heat transfer formulations, it can be shown that the reduced form of the entropy production equation can be written as

$$(23) \quad \dot{P}_s = \frac{\lambda}{T^2} \left(\frac{dT}{dz} \right)^2 + \frac{\mu}{T} \left(\frac{du}{dz} \right)^2 + \frac{i_y^2}{\sigma_e T}$$

Define the following non-dimensional entropy production, \dot{P}_s^* , and wall temperature,

$$(24) \quad \dot{P}_s^* = \frac{\dot{P}_s}{\lambda/a^2}, \quad \theta_w = \frac{\lambda T_w}{\mu u_B^2}$$

Using these variables, the non-dimensional entropy production equation becomes

$$(25) \quad \dot{P}_s^* = \frac{\left(\frac{d\theta}{dz} \right)^2}{(\theta + \theta_w)^2} + \frac{\left(\frac{du}{dz} \right)^2}{\theta + \theta_w} + \frac{i_y^2}{\theta + \theta_w}$$

In the following section, sample results of these analytical formulation will be presented.

Nanofluid and ferrofluid ferrofluid flow in minichannels

The term nanofluid describes a solid-liquid mixture that consists of nanoparticles and a base liquid. This is one of the new challenges for thermo-sciences provided by nanotechnology. The possible application area of nanofluids is in advanced cooling systems, micro/nano electromechanical systems and many others. The investigation of the effective thermal conductivity of liquids with nanoparticles has attracted much recent interest experimentally and theoretically. The effective thermal conductivity of nanoparticle suspensions can be much higher than for a fluid without nanoparticles. In our case we have calculated mixture of reference fluid and nanofluid particles as one phase fluid flow. The thermodynamic properties of nanofluids we have calculated with statistical thermodynamics.

Ferrofluids are based on magnetic nanoparticles that are so small, they contain only a single magnetic domain.

Conservation of energy:

$$(26) \quad \nabla^2 T + \frac{\dot{q}}{\lambda} = \frac{\rho c_p}{\lambda} \frac{\partial T}{\partial t}$$

After simplification we obtain:

$$(27) \quad \frac{\partial p}{\partial z} = \mu \frac{1}{r} \frac{\partial}{\partial r} \left(r \frac{\partial v_z}{\partial z} \right)$$

If we make a final simplification that the temperature gradient is linear, we obtain:

(28)

$$\frac{\partial T}{\partial z} = \frac{\dot{q}}{\rho c_p v_z}$$

Fluid dynamics:

We have studied a steady state condition in the circular tube. With these assumptions Navier-Stokes equation transforms into:

(29)

$$\frac{\partial p}{\partial z} = \mu \frac{1}{r} \frac{\partial}{\partial r} \left(r \frac{\partial v_z}{\partial z} \right)$$

If we assume a no-slip condition at the boundary surface and finite fluid velocity at the center of channel we obtain:

(30)

$$v_z = -\frac{R^2}{8\mu} \frac{\partial p}{\partial z} \left(1 - \left(\frac{r}{R} \right)^2 \right)$$

Magnetic Pressure:

If we consider the impact of magnetic field on the ferrofluid. According to reference we could express the influence of magnetic pressure with the next equation:

$$(31) \quad \frac{\partial p}{\partial z} = -\frac{1}{2} \mu_0 H \frac{\partial M}{\partial T} \frac{\partial T}{\partial z}$$

In the upper equation presents $\partial M / \partial T$ pyromagnetic effect and H is the field strength. To achieve the greatest pressure gradient it is desirable to maximize the pyromagnetic effect. The pyromagnetic effect has the biggest value at the Curie point.

Results and Discussion

Predicted results are illustrated in Figs. 2 – 6. In Fig. 3, the fluid viscosity decreases at lower temperatures. For fluid motion in microchannels, viscous dissipation in the streamwise direction generates internal energy. This creates a temperature rise and corresponding lower viscosity in Fig. 2, which affects the resulting pressure loss and mass flow rate through the microchannel.

Viscous dissipation can have significance in microchannel flows, due to much higher surface to volume ratios than large-scale channels. Discrepancies of the predicted friction constant with macro-scale theory may arise due to neglected temperature variations that occur from viscous dissipation in microchannels. An average tube temperature may produce more reliable results than viscosity calculations based on the inlet temperature. However, the average fluid temperature is generally unknown before a solution is derived, as it involves the unknown velocity gradient through viscous dissipation in the thermal energy equation. As a result, analytical approximations of temperature changes based on expressions developed in sections 2 – 3 can serve useful purposes in those regards.

The predicted velocity profiles without thermomagnetic effects are shown in Fig. 2. As expected, parabolic profiles are obtained, similar to Poiseuille flow in tubes. Unlike predicted trends in Fig. 2, the near-wall velocity gradient increases at larger Hartmann numbers in Fig. 3. The Hartmann number represents a ratio between electromagnetic and viscous forces on the fluid. When the relative magnitude of viscous forces become larger (at smaller Hartmann numbers), the wall friction increases. But increasing electromagnetic forces (at larger Hartmann numbers) also lead to higher resistance of fluid motion. Thus, wall friction can be minimized by optimization of the Hartmann number and magnitude of the applied electromagnetic field within a microchannel. Fig. 5 shows the velocity profile in nanofluid flow. Fig. 6 shows velocity distribution for fluid flow with ferroparticles (Fe_3O_4 in oil).

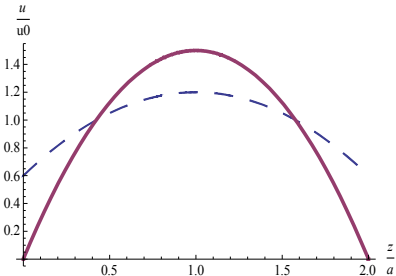


Fig. 2: Velocity profile without thermomagnetic effects, with ($\beta^*=0.5$) and without slip, in a rectangular microchannel

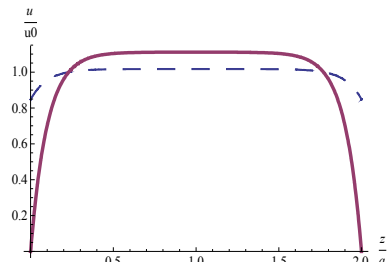


Fig. 3: Velocity profile (--- $M=10$, $\beta^*=0.5$, —— $M=10$, $\beta^*=0.0$) in a rectangular microchannel

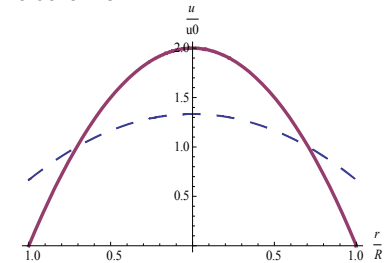


Fig. 4: Velocity profile without thermomagnetic effects, with ($\beta^*=0.5$) and without slip, in a circular microchannel

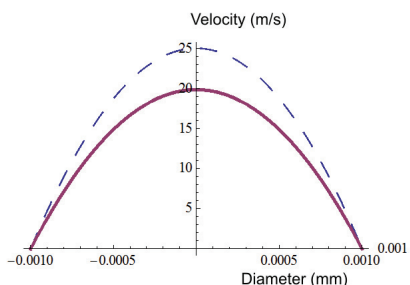


Fig 5: Velocity profile in pure water --- and water+ Al_2O_3 - $R=1$ mm

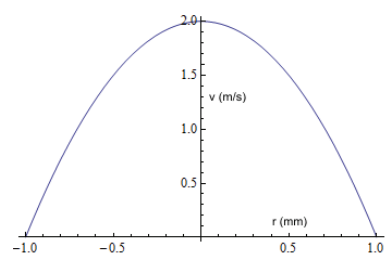


Fig 6: Velocity profile for oil with ferroparticles

REFERENCES

- [1] Zhao, C. Y., Lu, T. J., "Analysis of Microchannel Heat Sinks for Electronics Cooling", *International Journal of Heat and Mass Transfer*, vol. 45, no. 24, pp. 4857–4869, 2002.
- [2] Naterer, G. F., "Adaptive Surface Micro-Profilng for Microfluidic Energy Conversion" (to appear), *AIAA Journal of Thermophysics and Heat Transfer*, vol. 18, no. 3, 2004.
- [3] Gad-el-Hak, M., "The Fluid Mechanics of Microdevices – The Freeman Scholar Lecture", *ASME Journal of Fluids Engineering*, vol. 121, pp. 5 – 33, March 1999.
- [4] Israelachvili, J. N., "Measurement of the Viscosity of Liquids in Very Thin Films", *Journal of Colloid and Interface Science*, vol. 11, no. 1, pp. 263 – 271, 1986
- [5] Anderson, J. L., Quinn, J. A., "Ionic Mobility in Microcapillaries", *Faraday Transactions I*, vol. 68, pp. 744 – 748, 1972.
- [6] Migun, N. P., Prokhorenko, P. P., "Measurement of the Viscosity of Polar Liquids in Microcapillaries", *Colloid Journal of the USSR*, vol. 49, no. 5, pp. 894 – 897, 1987.
- [7] Pfahler, J., Harley, J., Bau, H., Zemel, J. N., "Gas and Liquid Flow in Small Channels", *Symposium on Microelectromechanical Sensors, Actuators and Systems*, vol. 32, pp. 49 – 60, 1991
- [8] Sharipov, F., "Rarefied Gas Flow through a Long Rectangular Channel", *Journal of Vacuum Science and Technology A*, vol. 17, no. 5, pp. 3062 – 3066, 1999.
- [9] Xu, B., Ootaki K. T., Wong N. T., Choi W. K., "Experimental Investigation of Flow Friction for Liquid Flow in Microchannels", *International Communications in Heat and Mass Transfer*, vol. 27, no. 8, pp. 1165 – 1176, 2000
- [10] Toh, K. C., Chen X. Y., Chai, J. C., "Numerical Computation of Fluid Flow and Heat Transfer in Microchannels", *International Journal of Heat and Mass Transfer*, vol. 45, no. 26, pp. 5133 – 5141, 2002.
- [11] Kim, S. J., Kim, D., Lee, D. Y., "On the Local Thermal Equilibrium in Microchannel Heat Sinks", *International Journal of Heat and Mass Transfer*, vol. 43, no. 10, pp. 1735 – 1748, 2000
- [12] Naterer, G.F., Effects of Thermomagnetic Irreversibilities on Microfluidic Transport, AIAA 2005-5327, 38th AIAA Thermophysics Conference, June 6-9 2005, Zoronto, Canada.
- [13] Naterer, G.F., Adeyinka O.B., Microfluidic exergy loss in a non-polarized thermomagnetic field, *International Journal of Heat and Mass Transfer*, Vol. 48 (2005), pp. 3945-3956.
- [14] Horiuchi, K., Dutta, P., Joule Heating Effects in Electroosmotically Driven Microchannel Flows, *International Journal of Heat and Mass Transfer*, Vol. 47 (2004), pp.:3085-3095.
- [15] Hetsroni, G., Mosyak, A., Pogrbnyak, E., Yarin, L.P., Fluid Flow in micro-channels, *International Journal of Heat and Mass Transfer*, Vol. 48 (2005), pp.:1982-1998.
- [16] White, F.M., *Fluid Mechanics*, McGraw-Hill, Fifth Edition, 2003, International Edition.
- [17] Aydin, O., Avci, M., Analysis of laminar heat transfer in micro-Poiseuille flow, *International Journal of Thermal Sciences*, vol. 46 (2007), pp.: 30-37.
- [18] Ngoma, G.D., Erchiqui, Heat flux effects on liquid flow in a microchannel, *International Journal of Thermal Sciences*, vol. 46 (2007), pp.: 1076-1083.
- [19] Rosenzweig, Ferrohydrodynamics, Dover, 1997.
- [20] Avsec, J., Oblak, M.. The calculation of thermal conductivity, viscosity and thermodynamic properties for nanofluids on the basis of statistical nanomechanics. *Int. j. heat mass transfer*. [Print ed.], Oct. 2007, vol. 50, iss. 21/22, str. 4331-4341.

Authors: prof. dr. Jurij Avsec, University of Maribor, Faculty of Energy Technology, Hocevarjev trg 1, 8270 Krsko, E-mail: jurij.avsec@uni-mb.si; Ass. prof.dr. Peter Virtic, University of Maribor, Faculty of Energy Technology, Hocevarjev trg 1, 8270 Krsko, E-mail: peter.virtic@uni-mb.si, prof. Dr. Greg F. Naterer, Canada Research Chair Professor, Faculty of Engineering and Applied Science, University of Ontario Institute of Technology, 2000 Simcoe Street North, Oshawa, Ontario, Canada, L1H 7K4, E-mail: greg.naterer@uoit.ca